Journal of Hazardous Materials 430 (2022) 128457

Contents lists available at ScienceDirect

Journal of Hazardous Materials

journal homepage: www.elsevier.com/locate/jhazmat

Effects of *ZmHIPP* on lead tolerance in maize seedlings: Novel ideas for soil bioremediation

Langlang Ma [a,1], Rong An [a,1], Li Jiang [a], Chen Zhang [a], Zhaoling Li [a], Chaoying Zou [a], Cong Yang [a], Guangtang Pan [a], Thomas Lübberstedt [b], Yaou Shen [a,*]

[a] State Key Laboratory of Crop Gene Exploration and Utilization in Southwest China, Maize Research Institute, Sichuan Agricultural University, Chengdu 611130, China
[b] Department of Agronomy, Iowa State University, Ames, IA, USA

HIGHLIGHTS

- A novel gene *ZmHIPP* controlling Pb-tolerance in maize was identified by QTL mapping and WGCNA.
- *ZmHIPP* was confirmed to modulate Pb-tolerance in maize, Arabidopsis, and yeast.
- *ZmHIPP* improves Pb deposition in the cell wall, alleviating Pb toxicity in maize.
- The polymorphism (A/G) in *ZmHIPP* promoter contributes to the difference in Pb-tolerance among maize lines.

GRAPHICAL ABSTRACT

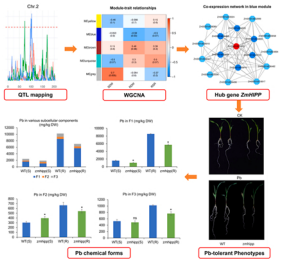

ARTICLE INFO

Keywords:
Pb tolerance in maize
Heavy-metal-associated isoprenylated plant protein
WGCNA
Linkage mapping
Functional validation

ABSTRACT

Extensive lead (Pb) absorption by plants affects their growth and development and causes damage to the human body by entering the food chain. In this study, we cloned *ZmHIPP*, a gene associated with Pb tolerance and accumulation in maize, using combined linkage mapping and weighted gene co-expression network analysis. We show that *ZmHIPP*, which encodes a heavy metal-associated isoprenylated plant protein, positively modulated Pb tolerance and accumulation in maize seedlings, Arabidopsis, and yeast. The genetic variation locus (A/G) in the promoter of *ZmHIPP* contributed to the phenotypic disparity in Pb tolerance among different maize inbred lines by altering the expression abundance of *ZmHIPP*. Knockdown of *ZmHIPP* significantly inhibited growth and decreased Pb accumulation in maize seedlings under Pb stress. *ZmHIPP* facilitated Pb deposition in the cell wall and prevented it from entering the intracellular organelles, thereby alleviating Pb toxicity in maize seedlings. Compared to that in the mutant *zmhipp*, the accumulated Pb in the wild-type line mainly consisted of the low-toxicity forms of Pb. Our study increases the understanding of the mechanism underlying Pb tolerance in maize and provides new insights into the bioremediation of Pb-polluted soil.

1. Introduction

Heavy metals were defined as those metals with a density greater than 5.0 g/cm^3, including thirty-eight elements (Passow et al., 1961). Among them, nonessential heavy metals like lead (Pb), cadmium (Cd), mercury (Hg), and aluminum (Al) are not required for the metabolic

* Corresponding author.
E-mail address: shenyaou@sicau.edu.cn (Y. Shen).
[1] These authors contributed equally to this work

https://doi.org/10.1016/j.jhazmat.2022.128457
Received 24 September 2021; Received in revised form 28 January 2022; Accepted 7 February 2022
Available online 11 February 2022

processes of plants (Hasan et al., 2009). Due to the environmental deterioration, industrial development, and sewage discharge, heavy metals have risen to important threats in agricultural production. Excessive heavy metals are poisonous and can cause damage to most living organisms (Antonovics et al., 1971). Owing to its nutritional value and high yield, maize (*Zea mays* L.) is used as a staple food, animal feed, and industrial crop worldwide (Godfray et al., 2010). According to the surveys conducted by the Food and Agriculture Organization, the global demand for maize production has steadily increased over the past few decades. As a highly persistent heavy metal, Pb has an estimated soil-maintenance time of 150–5000 years and has been one of the most frequently encountered heavy-metal pollutants of the environment (Gisbert et al., 2003). Excessive Pb affects the growth and development of maize by accumulating in roots, stems, leaves, and other organs (Shen et al., 2013; Zhang et al., 2017). More seriously, Pb stress leads to the yield and quality loss of maize (Dey et al., 2007). In addition, Pb can enter human and animal bodies via the food chain, causing irreversible damage to internal organs (Lippmann, 1990; Yang et al., 2000).

Plant roots absorb heavy metals from the soil and transport them to the stems, leaves, and grains via long-distance transportation, affecting plant growth and development (Nagajyoti et al., 2010). Excessive Pb is toxic to maize roots and inhibits the elongation of radicle cells (Obroucheva et al., 1998). Furthermore, Pb excess damages plant seedlings, mainly by changing cell membrane permeability, inducing leaf chlorosis, and affecting plant height and biomass (Tung and Temple, 1996). After entering plant cells, Pb chelates other substances, changes enzyme activities, and modifies the cell structure. Pb ions damage the chloroplast structure and disrupt chlorophyll synthesis, impacting photosynthesis (Cox et al., 1996; Ewais, 1997). When exposed to increased Pb concentrations, maize seedlings display an active superoxide system, including enhanced superoxide dismutase and peroxidase activities. Active oxygen causes cell death and irreversible damage to plants (Dietz et al., 2016).

When exposed to high concentrations of heavy metals, plants initially resist the exposure via the cell wall and leaf trichome (Kulich et al., 2015). Once the heavy metal ions are absorbed, plant cells produce metallothionein and transport them toward the vacuoles to protect the organelles (Ma et al., 2003). In Arabidopsis, the ABC transporter AtPDR8 (Kim et al., 2007), NRT1 family members NRT1.1 and NRT1.8 (Mao et al., 2014; Li et al., 2011), VirE2-interacting protein VIP1 (Tsugama et al., 2013), and heavy metal-associated isoprenylated plant proteins (HIPPs) (Tehseen et al., 2010) modulate heavy metal tolerance by binding to or transporting heavy metal ions. The vitamin E-deficient mutant *vte1* was more sensitive to copper (Cu) and Cd than wild-type (WT) Arabidopsis (Collin et al., 2008). Enhanced glutathione synthesis in Arabidopsis plays a role in mitigating the risk of reactive oxygen species induced by Cd stress (van de Mortel et al., 2008). In rice, OsHIPP41, STAR1/2 (an ABC transporter), and OsMTP11 (metal tolerance protein 11) play key roles in regulating the heavy metal tolerance (de Abreu-Neto et al., 2013; Farthing et al., 2017; Huang et al., 2009). Meanwhile, the metal-nicotianamine transporter OsYSL2 controls the translocation of manganese (Mn) and iron (Fe) into rice grains (Koike et al., 2004). The multidrug and toxic compound extrusion (MATE) contributes to sorghum resistance to Al (Magalhaes et al., 2007). In maize, the transcription factor ZmWRKY4 regulates the antioxidant defense caused by Cd stress (Hong et al., 2017). Recently, a P-type ATPase heavy metal transporter ZmHMA3 was reported to regulate Cd accumulation in maize kernels (Tang et al., 2021).

Several Pb transport-related genes have been reported in Arabidopsis. The ABC transporter AtPDR12 acts as a pump to exclude Pb^{2+} and/or Pb^{2+}-containing toxic compounds from the cytoplasm and confers Arabidopsis tolerance to Pb stress (Lee et al., 2005). The *PSE1* gene that encodes a NC domain-containing protein was proposed to mediate Pb tolerance partially through activating the ABC transporter *AtPDR12* (Fan et al., 2016). The *EIN2* gene was indicated to mediate Pb resistance at least in part through a GSH-independent AtPDR12-mediated mechanism (Cao et al., 2009). The acyl-CoA-binding protein ACBP1 binds to Pb^{2+} and mediates Pb accumulation in the shoots, conferring Pb tolerance in Arabidopsis (Xiao et al., 2008). However, limited studies have focused on the genes responsible for Pb tolerance in maize.

Quantitative trait loci (QTL) mapping depends on the genetic variations between the parents and among their recombinant offspring (Raihan et al., 2016; Wen et al., 2014). Considerable genetic variation is observed between different maize germplasms, more abundant than that between humans and chimpanzees (Buckler and Stevens, 2006; Yang et al., 2019). This facilitates the identification of the QTL responsible for the agronomic traits in maize. Using QTL mapping, researchers have recently identified numerous genetic loci for heavy metal tolerance and accumulation in maize. In a recombinant inbred line (RIL) population, 11 QTL intervals controlled arsenic (As) accumulation in maize leaves, stems, bracts, and kernels (Ding et al., 2011). Using another RIL population, 23 QTL were found responsible for mercury (Hg) accumulation, which explained 6.44–26.60% of the phenotypic variations (Fu et al., 2014). Additionally, 14 QTL controlling As accumulation in maize kernels were detected in this RIL population (Fu et al., 2016). Traditionally, to further map the heavy metal-regulating genes from the QTL intervals, QTL fine-mapping based on an enlarged recombinant population and increased marker density should be performed (Han et al., 2020). The weighted gene co-expression network analysis (WGCNA) enables the identification of hub genes in co-expression modules based on the gene expression patterns from RNA-seq data (Langfelder and Horvath, 2008). The module associated with target traits is selected by calculating the correlation between each module and the target traits (Li et al., 2021). Moreover, genome-wide association studies (GWAS) and WGCNA have been combined to successfully identify the potential functional genes responsible for salt tolerance in maize (Li et al., 2021; Ma et al., 2021).

This study performed QTL mapping in a maize RIL population to detect the QTL and candidate genes regulating Pb tolerance in maize seedlings. WGCNA was conducted with the expression abundances of these genes to construct the trait-associated co-expression modules. The hub gene (*ZmHIPP*), located in the associated module, was verified by candidate gene association analysis. *ZmHIPP* was subsequently functionally validated by heterologous expression in yeast and Arabidopsis and mutagenesis in maize. Our study revealed that *ZmHIPP* affected Pb accumulation and conferred Pb tolerance in maize seedlings. The identified superior haplotype of the *ZmHIPP* promoter contributes to molecular marker-assisted breeding of maize with improved Pb tolerance.

2. Materials and methods

2.1. Plant materials and phenotypic investigations

The 200 maize RILs used for QTL mapping were derived from the IBM Syn10 DH population that had high recombination frequency and was constructed from the parental lines B73 and Mo17 (Jansen et al., 2015). The genetic linkage map of the population has a total length of 1767.45 cM with an average distance of 0.29 cM between two adjacent markers (Ma et al., 2018).

To evaluate the phenotypes of these RILs, 30 seeds of each line were immersed in 10% H_2O_2 for 15 min and then rinsed twice with double-distilled water. These sterilized seeds were rolled up in germination paper (Anchor Paper, St. Paul, MN, USA) and vertically placed in a small bucket filled with double-distilled water (Ma et al., 2020). For each line, 12 growth-consistent seedlings were selected at the bifoliate stage and equally divided into two groups. One group was transferred into the Hoagland solution (CK) (Hou et al., 2021) and the other into the Hoagland solution containing 3 mM Pb^{2+} (T) (Shen et al., 2013; Gao et al., 2015). The seedlings were then cultured in a growth chamber with a photoperiod of 8/16 h (darkness/light) at 22/25 °C. The RIL population was grown in a randomized complete block design with three biological replicates. The shoot dry weight (SDW) and root dry weight (RDW) for each line were measured on the 14th day of culture. Since

heavy metal accumulation in plants changes the root-shoot ratio (RSR) (Xu et al., 2018), we incorporated it as an index for evaluating Pb tolerance. Pb tolerance for each trait was evaluated by calculating the lead-tolerance coefficient (LTC), which is equal to the ratio of the phenotypic value under Pb treatment (T) and that under normal conditions (CK) (Hou et al., 2021). For instance, the formula for calculating the LTC of SDW is as follows: LTC-SDW = SDW under T/SDW under CK.

2.2. QTL mapping of LTC traits and candidate gene identification

The QTL Cartographer v. 2.5 software (Wang et al., 2012) was used for QTL mapping based on composite interval mapping (CIM), with a 10-cM window size and a 1-cM walking speed. The logarithm odds (LOD) scores for these LTC traits were determined with 1000 permutations at a 0.05 significance level (Lander and Kruglyak, 1995). The naming rules of QTL were *q* followed by the LTC trait and the QTL sequential number. For example, in *q*LTC-SDW2, "*q*" denotes the QTL, LTC-SDW is the LTC for SDW, and the number "2" represents chromosome 2. The gene models located in the confidence intervals of these detected QTL were identified as the potential candidate genes responsible for Pb tolerance in maize seedlings.

2.3. RNA-Seq and WGCNA

To obtain the expression abundances of the identified candidate genes, we selected two lines with contrasting Pb tolerance for transcriptome sequencing under CK and Pb treatment conditions. The seedlings of the two lines SCL177 (Pb-sensitive) and SCL280 (Pb-tolerant) were cultured under CK and Pb for 72 h, as described in Section 2.1. For each line, the samples were individually collected from the roots of three seedlings at 0, 24, 48, and 72 h under CK and Pb stress, with three biological repeats. Meanwhile, SDW, RDW, and RSR for the two lines were investigated at various stages in each condition. A total of 42 samples were subjected to transcriptome sequencing, considering that the samples from the 0 h stage under CK were the same as those from the 0 h stage under treatment. Total RNA was isolated from these samples using TRIzol (Invitrogen, Gaithersburg, MD, USA) according to the manufacturer's instructions. Transcriptome sequencing reactions were carried out using the Illumina sequencing platform.

High-quality reads were obtained by filtering the raw reads using the fastp software and were subsequently aligned to the B73 RefGen_V4 reference genome (http://www.gramene.org) (Zhang et al., 2021a). Transcript levels were calculated using the mapped reads and were normalized to transcripts per kilobase million (TPM) using a consumer script. Among the candidate genes identified by QTL mapping, the differentially expressed genes (DEGs) were detected by calculating the absolute value of $\log_2$(fold change) between each Pb treatment stage and its corresponding CK stage. Subsequently, the TPM of the DEGs was subjected to WGCNA using the package WGCNA in R studio (Langfelder and Horvath, 2008). The co-expression modules were obtained with the following set of running parameters: variance data expression > 0, no missing data expression < 0.1, soft threshold (estimate value) = 10, deep split = 2, min module size = 8, and merge cut height = 0.25. The eigengene value of each module was applied to test the association between the module and the traits (SDW, RDW, and RSR) under Pb treatment and CK conditions. The significance threshold was set at P = 0.05 to identify the significantly associated modules. In each associated module, the genes with absolute eigengene-based connectivity value (|KME|) > 0.6 and topological overlap measure (TOM) > 0.2 were considered the hub genes. The key gene responsible for Pb tolerance was selected from the hub genes according to the functional annotation. Finally, Cytoscape software was used to draw the regulatory network for each associated module (Shannon et al., 2003).

2.4. Gene-based association analysis and ZmHIPP promoter activity assay

The key gene in the associated module was subjected to a gene-based association study. We used PCR to amplify the gene body and a 2000 bp upstream fragment from the genomic DNA of the 77 inbred lines with diverse genetic backgrounds. DNAMAN software (v5.2.2) was used for sequence alignment between the amplified sequences and the B73 genome to detect sequence polymorphisms, namely single nucleotide polymorphisms (SNPs) and insertion-deletions (InDels) (Ma et al., 2021). Combining the LTC phenotypes of the 77 lines, these SNPs and InDels were used to analyze the associations with LTC traits based on the generalized linear model (GLM) in the TASSEL v. 5.0 software (Zhang et al., 2021b). The significance threshold was set at P = 0.05, and the LD between the markers was calculated using HaploView software (http://www.broad.mit.edu/mpg/haploview). The haplotypes were divided according to the significant markers detected in the gene body and its 2000 bp upstream fragment. For each trait, a higher-LTC haplotype was identified as the superior haplotype for Pb tolerance.

The promoter sequence of *ZmHIPP* was amplified from a haplotype I-line SCL109 and a haplotype II-line SCL282 and separately inserted the upstream of the reporter gene *LUC* on the vector pGreenII-0800. The two recombinant plasmids contained the *Renilla luciferase* (*REN*) gene under the control of *35S* promoter, which was used as an internal reference to normalize the *LUC* expression level. The two constructs were then separately transformed into *Nicotiana tabacum* leaves by *Agrobacterium* injection. At 48 h of infection, the LUC and REN activities were measured by the Dual Luciferase Reporter Gene Assay Kit (Yeasen, Shanghai).

2.5. Phylogenetic analysis of ZmHIPP

ZmHIPP homologs were identified by the BLASTp program using the ZmHIPP amino acid sequence as a query in the NCBI database (http://www.ncbi.nlm.nih.gov/BLAST). Multiple alignment of these homologs was carried out using the ClustalW tool with the parameters "outfmt 7-evalue 1e-5." A phylogenetic tree was constructed using the neighbor-joining method in the MEGA v.6.0 software, and the bootstrap value was set to 1000 to test the confidence of topology (Li et al., 2011).

2.6. Expression, purification, and structural analysis of ZmHIPP

The coding sequence (CDS) of *ZmHIPP* was cloned from line B73 and inserted into the prokaryotic expression vector pET-28a. The recombinant construct was subsequently transformed into the *Escherichia coli* BL21 (DE3) strain. The His-ZmHIPP fusion protein was induced at 15 °C with 0.5 mM isopropyl-β-D-thiogalactoside and was purified by the Ni-NTA-Sefinose Column (Sangon, Shanghai, China). Circular dichroism (CD) analysis was used to dissect the secondary structure of ZmHIPP, which was carried out on the Chirascan-Plus CD spectrophotometer (Applied Photophysics, UK) at 25 °C. The data obtained from wavelength of 190–260 nm were subjected to CNDD software (version 2.1, Applied Photophysics Ltd., Leatherhead, UK) for calculating the secondary structure compositions (Li et al., 2018a).

2.7. qRT-PCR of ZmHIPP in different haplotype lines

Using an ABI 7500 real-time PCR System (Torrance, CA, USA), real-time quantitative PCR (qRT-PCR) was carried out to test the expression of *ZmHIPP* under Pb treatment in different haplotype lines. Total RNA was extracted from the roots of different lines 24 h after treatment with 3 mM Pb^{2+}, using the TRIzol reagent (Invitrogen, Gaithersburg, MD, USA). The PrimeScriptTMRT reagent kit (TaKaRa, Japan) was used for cDNA synthesis; qRT-PCR was carried out using 200 nM of the gene-specific primer pairs (Table S1) with 10 ng of cDNA and 10 μL of SYBR Green Supermix (Bio-Rad, USA). The PCR was performed in an

ABI 7500 real-time PCR System as per the following conditions: an initial step at 95 °C for 10 min to denature the DNA, followed by 35 cycles of 98 °C for 5 s, 60 °C for 10 s, 94 °C for 30 s, and a final step at 60 °C for 30 s. Each reaction was performed in triplicate with *ZmActin 1* (*GRMZM2G126010*) as the reference gene. The $2^{-\triangle\triangle CT}$ method was used to calculate the relative expression levels of *ZmHIPP* in different samples.

2.8. Subcellular localization

The CDS of *ZmHIPP* without the stop codon was cloned from line B73 and inserted into an eGFP vector under the control of a *35S* promoter, to generate the recombinant plasmid *p35S:ZmHIPP-eGFP*. The fusion construct was transformed into the protoplasts of maize leaves using PEG4000. The transformed protoplasts were examined for eGFP fluorescence under a confocal microscope (ZEISS LSM800, Germany) 48 h after culturing under low light at 28 °C. The subcellular localization of ZmHIPP was also examined by the transient expression of *p35S:ZmHIPP-eGFP* in tobacco leaves via an *Agrobacterium* injection.

2.9. Heterologous expression of ZmHIPP in yeast

Yeast strains, including the Pb-sensitive mutant strain Δycf1 and the WT strain BY4741, were used in this study. The full-length CDS of *ZmHIPP* was cloned from line B73 and inserted into the pYES2 vector driven by the *GAL1* promoter, to produce the recombinant construct *pGAL1:ZmHIPP*. The construct was transformed into the mutant Δycf1 strain by electroporation, and the transformed strain was incubated on solid YPD medium with or without 30 μM Pb^{2+} (Holland et al., 2013) at 30 °C for 3 d. The Δycf1 strain transformed with pYES2 and the WT strain BY4741 were used as the negative and positive controls, respectively. The OD_{600} of the yeast cultures at 0, 12, 24, 36, 48, 60, 72, and 84 h was measured to determine the growth of these transformants. The Pb content in the yeast cells was measured using inductively coupled plasma-mass-spectrometry (ICP-MS; NexION 2000, PerkinElmer Inc.) at 72 h after liquid incubation of 20 μM, 30 μM, 60 μM, and 90 μM Pb^{2+}, respectively.

2.10. Overexpression of ZmHIPP in Arabidopsis

The full-length CDS of *ZmHIPP* was inserted into the vector pRI 101-AN driven by *35S* promoter. The recombinant construct *p35S:ZmHIPP* was introduced into the *Agrobacterium* strain GV3101 and was used to transform *Arabidopsis thaliana* WT Columbia (Col) using the floral-dip method (Clough and Bent, 2010). Positive transgenic lines were identified by a combination of *ZmHIPP*-specific PCR and kanamycin-resistant screening. Homozygous transgenic lines for Pb tolerance evaluation were obtained after three generations of self-pollination.

Seeds from the transgenic and Col lines were surface-sterilized, plated on half-strength MS medium with 200 mg/L Pb^{2+} (Pb treatment) (Zhang et al., 2017) or without supplemented Pb^{2+} (CK), and cultured at 22 °C for 15 d. The root length and biomass were individually investigated on day 15.

2.11. Evaluation of Pb tolerance in the maize mutant zmhipp

The UniformMu mutant (*zmhipp*, stock number: UFMu-01490) of *ZmHIPP* was obtained from the MaizeGDB database (https://www.maizegdb.org/). The background of the mutant is W22, and a Mu transposon is located within the 5′-UTR of *ZmHIPP*. After three generations of self-pollination, the homozygous mutant *zmhipp* was identified via *TIR6* and *zmhipp*-specific PCR with the primer pairs described in Table S1. Furthermore, qRT-PCR was used to detect the expression level of *ZmHIPP* in the WT and *zmhipp* lines using the primers listed in Table S1. Total protein was extracted from the roots of the WT and mutant plants using the Plant Total Protein Extraction Kit (Sangon, China). The sandwich ELISA was performed to detect the expression level of the ZmHIPP protein in the above lines. Briefly, each well was coated overnight at 4 °C with 8 μg protein. The plate was washed with PBST three times (3 min each time), blocked with the blocking buffer (5% non-fat milk powder) at 37 °C for 1 h, and then washed with PBST three times. Monoclonal antibody against ZmHIPP antigen (Sangon, China) dilution of 1:100 in PBS was added and incubated at 37 °C for 1 h. The wells were washed with PBST and incubated with the HRP-conjugated Goat Anti-Rabbit IgG diluted to 1:2000 PBS for 1 h at 37 °C. Plate was washed with PBST three times, incubated with 1% TMB for 15 min. The reaction was terminated by adding 2 M H_2SO_4 and plate was read at 450 nm with a microtiter plate reader (ThermoFisher Scientific, USA).

At the bifoliate stage, the Pb tolerance of the *zmhipp* line was evaluated using the method described in Section 2.1. In addition to SDW, RDW, and RSR, 10 root system architecture (RSA)-related traits were investigated in this study, namely total root length (TRL), primary root length (PRL), total secondary root length (TSRL), root perimeter (PER), root depth (DEP), standard root length (SRL), root volume (VOL), total surface area of root (TSA), root width (WID), and maximum number of roots (MNR). These RSA-related phenotypes were observed using the EPSON Expression 10000XL Root Scanner and evaluated by the ARIA software (Pace et al., 2014). The LTC for each trait, represented by the ratio of the phenotypic value under T to that under CK, was then calculated.

2.12. Elucidation of the mechanism underlying Pb tolerance in maize seedlings

To investigate the Pb tolerance mechanism mediated by *ZmHIPP*, we examined the total Pb content in the roots and shoots of the mutant *zmhipp* using ICP-MS. The Pb contents in different chemical forms and various subcellular components in the *zmhipp* and WT lines were compared.

To reveal the subcellular distribution of Pb, six plants were soaked in 0.02 M Na_2EDTA, rinsed with deionized water, and divided into root and shoot parts. In total, 0.5 g fresh material was homogenized in a pre-cooled extraction buffer (Wang et al., 2015). Cell components were separated into three fractions by differential centrifugation at 4 °C (Weigel and Jäger, 1980; Zhou et al., 2008). F1 was composed of cell walls and relative debris, F2 consisted of cell membranes and organelles, and F3 involved cytosol and cytoplasm.

Different chemical forms of Pb were individually extracted using a series of extractants: 1) 80% ethanol to extract inorganic Pb (nitrate/nitrite and chloride), 2) deionized water (dH_2O) to extract Pb-organic acid complexes of water solubility and $Pb(H_2PO_4)_2$, 3) 1 M NaCl to extract Pb pectates, protein-integrated Pb, and adsorptive Pb, 4) 2% acetic acid to extract insoluble Pb phosphate and other Pb phosphate complexes, and 5) 0.6 M HCl to extract Pb oxalate (Wang et al., 2015; Xu et al., 1991; Xu and Wang, 2013). Pb concentrations in various chemical forms were determined using ICP-MS.

2.13. Statistical analysis

The SPSS v. 20.0 software (http://www.spss.com) was used to calculate the correlations between traits and perform phenotypic statistics to obtain the mean value, standard deviation (SD), coefficient of variation (CV), skewness, and kurtosis for each trait. Analysis of variance (ANOVA) was conducted using SAS v. 9.3 software. The broad-sense heritability (H_B^2) values of these traits were individually estimated based on the method described by Pace et al. (2015). Differences were determined by a *t*-test at a p-value < 0.05.

3. Results

3.1. Phenotypic variations of Pb tolerance among the RIL population

To address the variations in Pb tolerance, SDW, RDW, and RSR were investigated in the IBM Syn10 DH population of maize under control (CK) and test (T) conditions. Under CK conditions, the average amounts of SDW, RDW, and RSR were 0.031 g, 0.026 g, and 0.906, respectively, with CVs of 0.337, 0.235, and 0.204, respectively (Table S2). Under T conditions, the average values of these three traits were 0.024 g, 0.021 g, and 0.947 among the 200 RILs, respectively, with CVs of 0.276, 0.237, and 0.194, respectively (Table S2). For each trait, a significant difference ($P < 0.05$) was observed between the CK and T groups, where SDW and RDW decreased and RSR increased under T conditions compared to their values under CK conditions (Fig. 1A, B, C). This suggests that Pb stress affected the phenotypes of the RIL population. The H_B^2 for each trait ranged from 61.36% to 84.49% and 56.54–79.10% under CK and T conditions, respectively (Table S2). This implies that the phenotypic variations were mainly genetically controlled under both conditions. Moreover, the phenotype frequencies of all traits were normally distributed (Fig. 1E, F), suggesting that quantitative loci controlled these traits. Correlation analysis showed that SDW and RDW had the highest correlation, with a correlation coefficient of 0.79 (CK) and 0.74 (T) (Fig. 1E, F), verifying that the development of the root system influences the growth of shoots in maize seedlings. To evaluate the Pb tolerance of the population, we calculated the LTC for each line. Among the different traits in the RIL population, the LTC of SDW was the lowest while that of RSR was the highest (Fig. 1D). This suggests that Pb stress had a bigger impact on SDW than on RDW and RSR.

3.2. QTL and candidate genes responsible for Pb tolerance in maize seedlings

A total of six QTL located on chromosomes 2, 4, 6, and 7 were identified using the LTC values of SDW, RDW, and RSR. The LOD value of each QTL ranged from 2.52 (*q*LTC-RSR6) to 3.13 (*q*LTC-SDW2), with their phenotypic variation explained (PVE) between 4.66% (*q*LTC-RSR6) and 5.93% (*q*LTC-SDW2) (Fig. S1, Table S3). No major QTL with PVE ≥ 10% were identified for these LTC values (Table S3), suggesting that multiple minor loci mainly controlled the Pb tolerance of maize seedlings. Four QTL (*q*LTC-SDW2, *q*LTC-SDW4, *q*LTC-SDW6, and *q*LTC-RDW7) had negative additive effects, indicating that the higher Pb tolerance of the shoots and roots was mainly derived from the Mo17 parent (Table S3). The physical distance of flanking makers for each QTL ranged from 0.70 Mb to 6.175 Mb (Table S3). Based on the QTL intervals, 267 gene models were identified, with 67, 20, 27, 21, 76, and 56 models resolved to *q*LTC-SDW2, *q*LTC-SDW4, *q*LTC-SDW6, *q*LTC-RDW7, *q*LTC-RSR2, and *q*LTC-RSR6, respectively (Table S4).

3.3. Hub genes identified from the candidate genes by WGCNA

To identify the hub genes from the candidate genes detected by QTL mapping, we carried out a WGCNA by combining the phenotypes and the corresponding expression levels of the 267 genes in two inbred lines with contrasting Pb tolerance. Under T conditions, phenotypic differences were observed between the two lines at each stage, except for SDW at 48 and 72 h and for RSR at 24 h (Fig. S2). Generally, under T conditions, the Pb-tolerant line SCL 280 showed higher SDW, RDW, and RSR than the Pb-sensitive line SCL177 (Fig. S2). Among the 267 candidate genes in line SCL177, 23, 15, and 18 genes were differentially expressed (with $|\log_2(\text{fold change})| > 1$, $Q < 0.05$) at 24, 48, and 72 h,

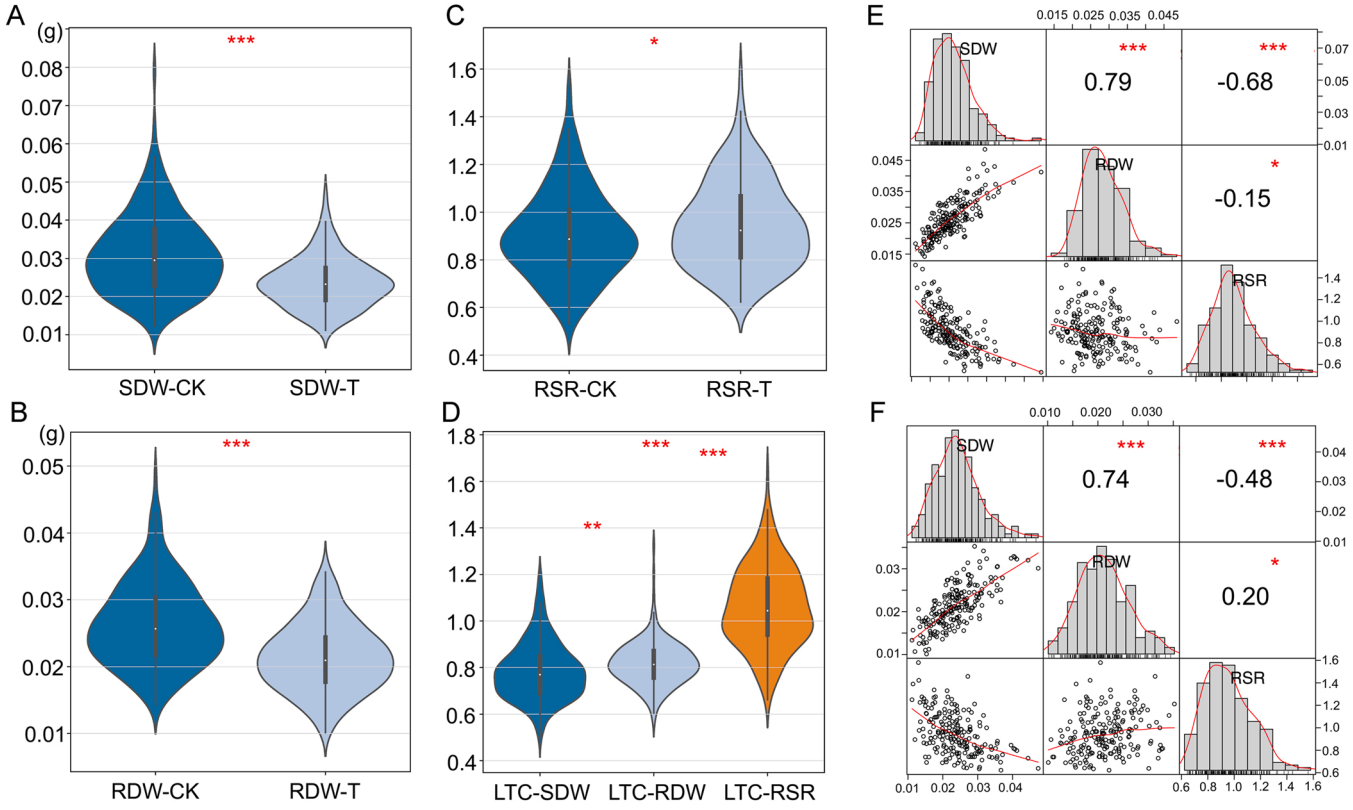

Fig. 1. Phenotypes of the IBM Syn 10 DH population under normal conditions (CK) and Pb treatment. (A), (B), and (C) Phenotypic values of shoot dry weight (SDW), root dry weight (RDW), and root-shoot ratio (RSR) for the population, respectively. (D) Phenotypic values of the lead-tolerance coefficients (LTCs) for the population. (E) and (F) Correlations between these three traits and their phenotypic distributions among the population under CK and Pb treatment. * , ** , and *** denote significant differences at $P < 0.05$, $P < 0.01$, and $P < 0.001$ levels, respectively.

respectively (Table S5). In line SCL280, 60, 6, and 15 of these candidate genes were differentially expressed at the three respective stages (Table S5). From the candidates detected by QTL mapping, we identified 82 genes responding to Pb stress in the two lines (Table S5).

Based on the expression abundance, 74 of the 82 genes were classified into four co-expression modules, namely blue (18), brown (17), turquoise (29), and yellow (10), whereas the remaining eight genes remained unclassified (in the grey module) (Fig. 2A). Moreover, correlation analysis between the modules and the phenotypes illustrated that only the blue module had a significant ($P < 0.05$) correlation with a trait (RDW) (Fig. 2B). Therefore, the blue module was considered the Pb tolerance-associated module, and seven genes with a $|KME| > 0.6$ and a $TOM > 0.2$ were identified as the hub genes. The functional annotations showed that the gene model *Zm00001d004931* encodes a heavy metal-associated (HMA) isoprenylated plant protein (HIPP). HMA is a conserved domain found in numerous proteins that transport or detoxify heavy metals (Leng et al., 2019). Therefore, *Zm00001d004931* (*ZmHIPP*) was the causal gene for manifesting Pb tolerance in maize seedlings. Under CK conditions, the *ZmHIPP* expression reached the peak at 48 h and 24 h of the seedling growth in SCL177 and SCL280, respectively (Fig. S3A). Under Pb stress, the *ZmHIPP* expression showed an increasing trend with the treatment process in both lines (Fig. S3B). Notably, the *ZmHIPP* expression value was higher in the Pb-tolerant line SCL280 than that in the Pb-sensitive line SCL177 at each Pb treatment period (Fig. S3B). Based on the node Cytoscape results from WGCNA, we constructed the regulatory network of *ZmHIPP* and its co-expressed genes in the blue module (Fig. 2C).

3.4. Genetic variation in the promoter of ZmHIPP affected the tolerance of maize to Pb stress

To investigate the potential function of *ZmHIPP*, we conducted a phylogenetic analysis of various plant species based on the amino acid sequences of the ZmHIPP homologs. A total of 391 genes from six plant species were identified as orthologs of *ZmHIPP*, including 45 in Arabidopsis, 39 in rice, 83 in wheat, 53 in sorghum, 74 in soybean, and 97 in maize. We constructed a phylogenetic tree using *ZmHIPP* and some of its orthologs (Fig. S4). Among them, three genes from sorghum (*Sobic.005G033700*, *Sobic.005G033400*, and *Sobic.005G033600*) and two from maize (*Zm00001d017393* and *Zm00001d023372*) showed the closest phylogenetic relationship with *ZmHIPP* (Fig. S4). Prokaryotic expression showed that the molecular weight of the ZmHIPP protein was ~ 60.00 kDa (Fig. S5A). CD analysis revealed that ~6.10%, ~17.20%, and ~29.70 of the amino-acid residues were in the α-helical, beta-turn, and random coil conformations, respectively (Fig. S5B).

To verify whether variations in *ZmHIPP* influence Pb tolerance, we performed an association analysis for *ZmHIPP* using the genotypes and LTC phenotypes of 77 inbred lines in maize (Table S6). Six SNPs were observed in the promoter and nine in the gene body of *ZmHIPP* (Table S7). Using the GLM, one SNP (S2_149356641, A/G) located in the promoter was significantly ($P < 0.05$) associated with LTC-SDW and LTC-RSR (Fig. 3A). T-tests showed that the lines with "A" allele had significantly ($P < 0.05$) higher LTC-SDW and lower LTC-RSR than those with "G" allele (Fig. 3B). To test whether the variation affected *ZmHIPP* expression among different lines, we randomly selected five "A"-type lines and five "G"-type lines for qRT-PCR analysis of *ZmHIPP* in roots under Pb treatment. The *ZmHIPP* expression level in the "A"-type lines was significantly higher than in the "G"-type lines after 24 h of Pb treatment (Fig. 3 C). In addition, the relative *LUC* activity of the "A"-type promoter was 28.56-fold higher ($P < 0.001$) than that in the "G"-type promoter, suggesting that the "A"-type promoter had a higher transcriptional activity than the "G"-type promoter (Fig. 3D). All these findings suggest that the "A/G" transition in *ZmHIPP* promoter controlled its expression abundance, thereby affecting the Pb tolerance

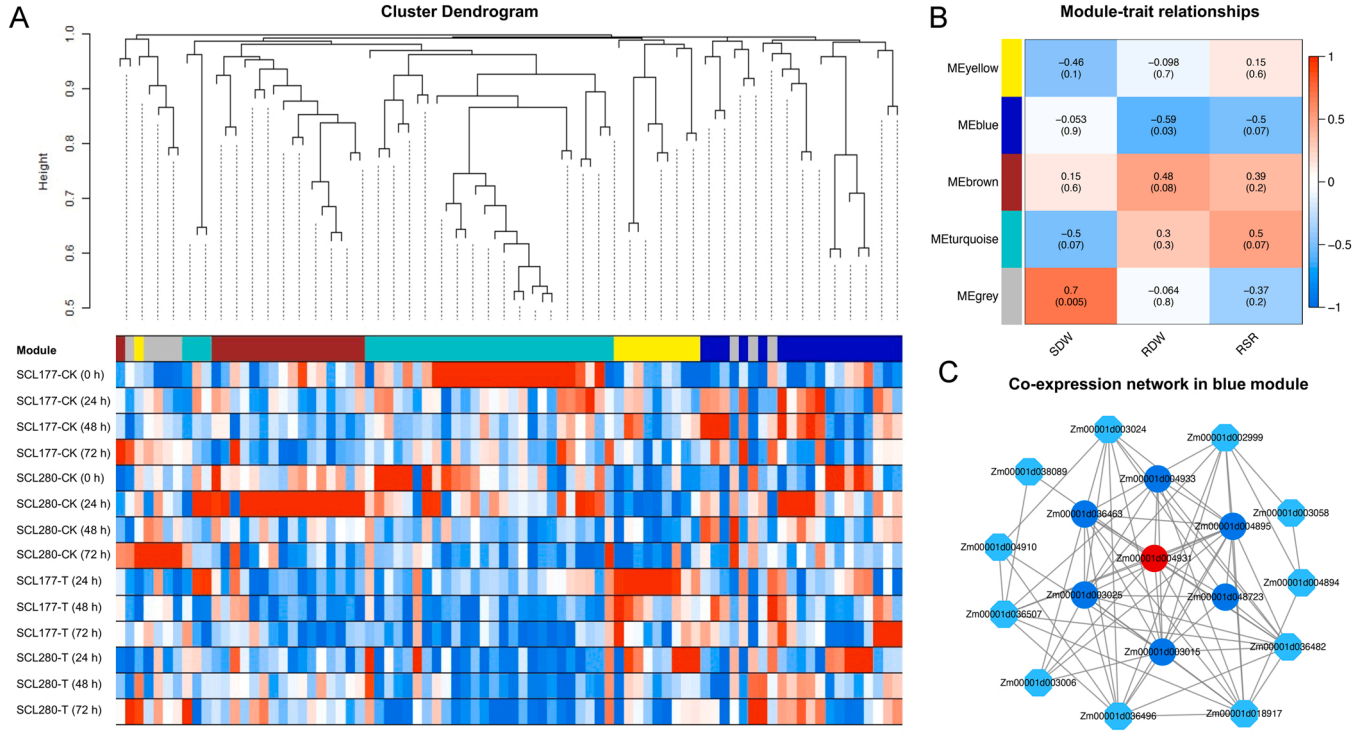

Fig. 2. Results of weighted gene co-expression network analysis (WGCNA) conducted using transcriptome data and phenotypes of seedling traits under Pb stress. (A) Co-expression modules identified by WGCNA. Brown, yellow, turquoise, and blue represent four co-expression modules; grey shows the unclassified transcripts according to their expression patterns. (B) Correlations between the modules and phenotypes. Numbers outside parentheses represent the correlation coefficients between the modules and phenotypes; numbers inside parentheses denote the P-values of the correlation coefficients. (C) Regulatory network constructed for the trait-associated module (blue module). The red circle shows the prioritized causal gene for Pb tolerance; dark blue circles display the other hub genes.(For interpretation of the references to colour in this figure, the reader is referred to the web version of this article.)

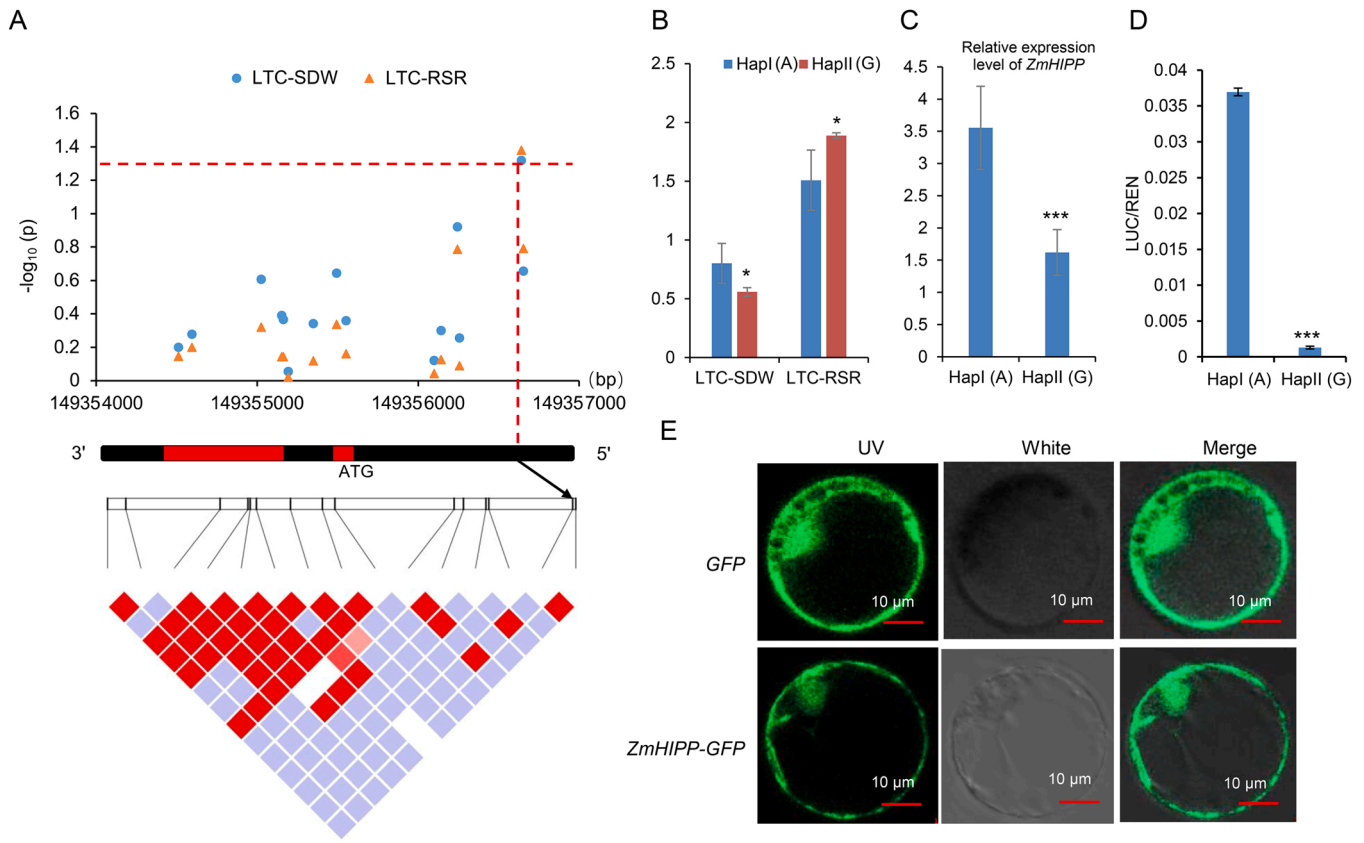

Fig. 3. Association analysis and subcellular localization for *ZmHIPP*. (A) Significant variations associated with lead-tolerance coefficients (LTCs) of seedlings. The red dotted line shows the threshold of significance (P = 0.05). LTC-SDW and LTC-RDW represent the LTCs of shoot dry weight and root dry weight, respectively. The structure of *Zm00001d004931* is shown in the middle; bold red lines represent the exons. Pairwise linkage disequilibrium between markers is displayed at the bottom. (B) Comparison of LTC-SDW and LTC-RDW between haplotypes. * denotes a significant difference between HapI and HapII at $P < 0.05$ level. (C) Expression levels of *ZmHIPP* in different haplotype lines. *** represents a significant difference between HapI and HapII at $P < 0.001$ level. (D) Comparison of the promoter activities between the two contrasting haplotypes. *** represents a significant difference between HapI and HapII at $P < 0.001$ level. (E) Subcellular localization of ZmHIPP in maize protoplasts.(For interpretation of the references to colour in this figure, the reader is referred to the web version of this article.)

of maize seedlings. Subcellular localization analysis using maize protoplasts and tobacco leaves demonstrated that the ZmHIPP-GFP fusion protein was localized in the nucleus and the cell membrane (Fig. 3E, Fig. S6).

3.5. Heterologous expression of ZmHIPP enhanced Pb tolerance in yeast and Arabidopsis

To investigate the role of *ZmHIPP* in Pb tolerance, we heterologously expressed *ZmHIPP* in a Pb-sensitive yeast strain Δycf1. Compared to that in the WT strain BY4741, the growth of Δycf1 strain was significantly inhibited in the medium containing 30 μM Pb^{2+} (Fig. S7). The recombinant Δycf1-*ZmHIPP* displayed higher Pb tolerance in the 30 μM Pb^{2+} medium than the Δycf1 strain transformed with pYES2 (negative control) (Fig. 4A, B). The yeast growth curve indicated that under Pb stress, the recombinant Δycf1-*ZmHIPP* had a faster growth rate than the Δycf1-pYES2 strain (Fig. 4C). However, no significant difference in Pb tolerance was observed between the two recombinants Δycf1-*ZmHIPP* and BY4741(WT)-pYES2 after 30 μM Pb^{2+} treatment (Fig. 4B), illustrating that the heterologous expression of *ZmHIPP* effectively complemented Pb tolerance in the mutant Δycf1. Additionally, Pb concentration in the recombinant Δycf1-*ZmHIPP* significantly increased by 129.26%, compared to that in the Δycf1-pYES2 strain (Fig. 4D). To further verify the role of *ZmHIPP* on Pb tolerance, we determined the Pb contents in the Δycf1-*ZmHIPP* under Pb^{2+} treatment concentrations of 20 μM, 60 μM, and 90 μM. The results showed that Pb concentration in Δycf1-*ZmHIPP* was significantly higher ($P < 0.001$) than that in the Δycf1-pYES2 strain after each of the Pb^{2+}-concentration treatments (Fig. S8). These findings suggest that *ZmHIPP* positively mediates Pb absorption in yeast cells.

ZmHIPP was transformed into Arabidopsis, generating three independent transgenic events that overexpressed the gene. Under CK conditions, no difference was observed in the root and shoot growth between the OE (overexpression) and WT lines (Fig. 4E, F, G). Under 200 mg/L Pb^{2+} treatment, the growth of the WT line was significantly inhibited compared to that of the OE lines. Compared to the average root lengths of WT plants under Pb stress, those of OE1, OE2, and OE3 lines increased by 29.69%, 30.10%, and 26.60%, respectively (Fig. 4E, F). The biomass of the three transgenic lines was 1.16-, 1.13-, and 1.21-fold higher than that of the WT line, respectively, when exposed to Pb treatment (Fig. 4E, G). These findings demonstrated that overexpression of *ZmHIPP* in Arabidopsis improved the Pb tolerance of Arabidopsis seedlings.

3.6. ZmHIPP positively regulates Pb accumulation and tolerance in maize seedlings

To validate the function of *ZmHIPP* in Pb tolerance in maize, we evaluated the biomass LTCs of the knockdown mutant (*zmhipp*) under Pb stress. qRT-PCR analysis showed that *ZmHIPP* expression in the homozygous mutant was only 0.13- and 0.33-fold lower than that in the WT (W22) line under normal conditions and Pb^{2+} treatment, respectively (Fig. S9A, B). ELISA supported that the expression of ZmHIPP protein was significantly ($P < 0.001$) downregulated in the mutant *zmhipp*

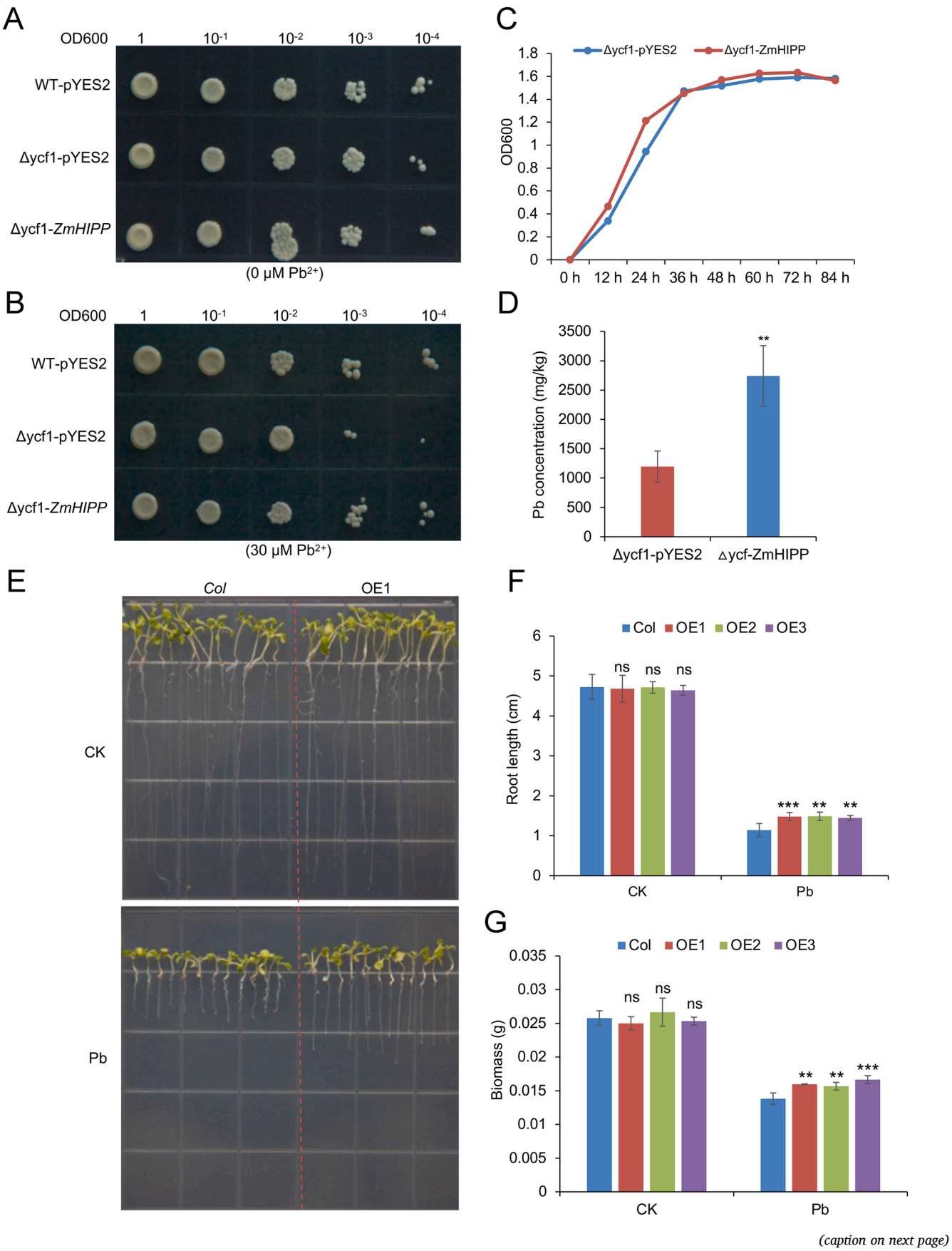

(caption on next page)

Fig. 4. Heterologous expression of *ZmHIPP* improves Pb tolerance in yeast and Arabidopsis. (A) Comparison of the growth rate between the wild-type (WT) yeast, the mutant (Δycf1-pYES2), and Δycf1 transformed with *ZmHIPP* (Δycf1-*ZmHIPP*) under normal conditions. (B) Comparison of the growth rate between WT, Δycf1-pYES2, and Δycf1-*ZmHIPP* strains under 30 μM Pb^{2+} treatment. (C) Growth curves of Δycf1-pYES2 and Δycf1-*ZmHIPP* strains under 30 μM Pb^{2+} treatment. (D) Comparison of Pb concentration in yeast cells between Δycf1-pYES2 and Δycf1-*ZmHIPP* strains under 30 μM Pb^{2+} treatment. (E) Comparison of the seedlings between the WT Arabidopsis (Col) and the transgenic line (OE1) under Pb stress (200 mg/L Pb^{2+}) for 15 d. (F) Root lengths of the transgenic lines OE1, OE2, OE3, and Col after 15 d of Pb treatment. (G) Biomass phenotypes of the transgenic lines OE1, OE2, OE3, and Col after 15 d of Pb treatment. CK, normal conditions; Pb, Pb treatment. ns represents no significance ($P > 0.05$) between Col and the OE line. ** and *** denote a significant difference between Col and the OE line at $P < 0.01$ and $P < 0.001$ levels, respectively.

compared with that in WT under both conditions (Fig. S9C, D). The reduced *ZmHIPP* expression in the mutant caused a significant ($P < 0.05$) decrease in the LTCs of both SDW and RDW, with LTC-SDW and LTC-RDW for the WT line being 0.995 and 0.960, respectively, and those of the mutant being 0.887 and 0.894, respectively (Fig. 5A, B, C, D, E, F). We measured the LTCs of 10 RSA traits in the mutant, which indicated that only the LTCs of TSRL and SRL were significantly ($P < 0.05$) decreased in the mutant as compared to those in the WT line (Fig. 5G, H). The other traits did not significantly differ in their LTCs between the mutant and the WT lines (Fig. S10). This suggested that *ZmHIPP* positively regulates Pb tolerance of maize roots by mainly affecting the length of secondary roots under Pb stress.

In both the mutant and WT lines, majority (80.598–81.384%) of Pb was retained in the roots, while only a small proportion (18.616–19.402%) was transported to the shoots (Fig. 5I). The Pb content in the roots of the mutant line was 67.854% lower than that in the roots of the WT line (Fig. 5I). Concurrently, Pb accumulation in the shoot of the mutant line was significantly ($P < 0.05$) decreased to 2531.433 mg/kg dry weight (DW) compared to the 3545.050 mg/kg DW in the WT line (Fig. 5I). These results indicated that *ZmHIPP* positively affects Pb uptake, translocation, and tolerance in maize seedlings.

3.7. *ZmHIPP facilitates Pb deposition in the cell wall and alleviates Pb toxicity in maize*

The chemical forms and subcellular distribution characteristics of Pb in plants affect Pb absorption and tolerance capacities (Wang et al., 2008). We focused on the subcellular distribution patterns and chemical forms of Pb in the WT (W22) and mutant (*zmhipp)* lines.

In the roots of both lines, Pb oxalate (extracted by 0.6 M HCl) was the major Pb-bearing component (58.30–60.05%), followed by undissolved Pb phosphate (extracted by 2% HAC), which was 17.46–20.28% of the total Pb (Fig. 6A). In the roots, Pb pectates, protein-integrated Pb, and adsorptive Pb (extracted by 1 M NaCl) had the lowest proportion (2.88–3.19%) (Fig. 6A). The roots of the WT plants showed significantly ($P < 0.05$) higher Pb concentrations across all chemical forms, except the water-soluble Pb in inorganic form (extracted by 80% ethanol), than the roots of the mutant line (Fig. 6B, C, D, E, F). Furthermore, compared to that in the mutant line, the increased Pb concentration in the roots of the WT line was mainly due to the presence of less toxic Pb forms, namely Pb oxalate and undissolved Pb phosphate (Fig. 6E, F). In the shoots of both lines, water-soluble Pb in inorganic form (35.36–36.75%) and Pb oxalate (33.921–34.570%) were the major forms of Pb, whereas the undissolved Pb phosphate had the smallest percentage (4.92–5.06%) (Fig. 6A). In contrast to that in the mutant shoots, the enhanced Pb

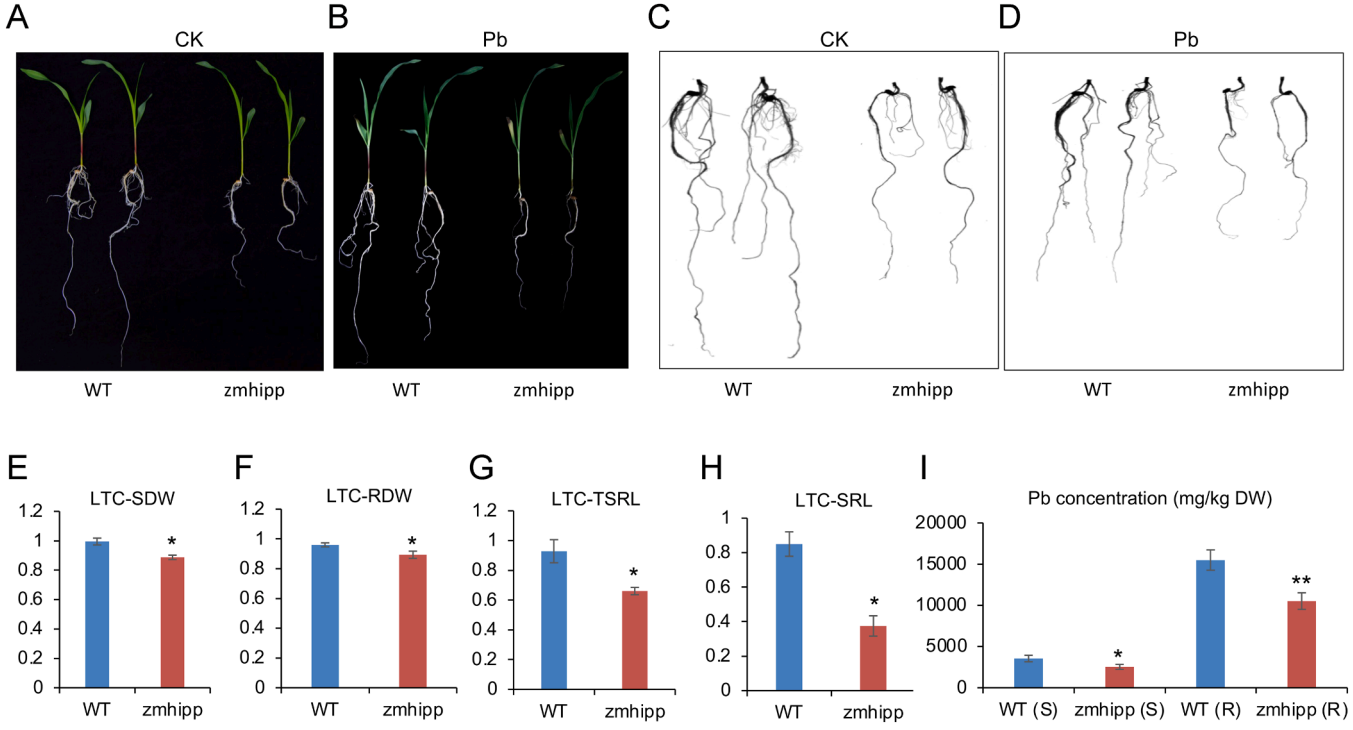

Fig. 5. Pb-tolerant phenotypes of the mutant *zmhipp*. (A) Phenotypic comparison between the wild-type (W22) and the mutant (*zmhipp*) under normal conditions. (B) Phenotypic comparison between W22 and *zmhipp* under 30 mM Pb^{2+} treatment. (C) and (D) Root system architecture (RSA) of W22 and *zmhipp* under normal conditions (CK) and 30 mM Pb^{2+} treatment, respectively. (E) and (F) Lead-tolerance coefficients (LTCs) of shoot dry weight (SDW) and root dry weight (RDW), respectively. (G) and (H) LTCs of the root system architecture (RSA)-related traits, total secondary root length (TSRL), and standard root length (SRL). (I) Pb concentration in W22 and *zmhipp* under Pb stress. * and ** denote significant difference between W22 and *zmhipp* at $P < 0.05$ and $P < 0.01$ levels, respectively. WT (S) and WT (R) represent the shoots and roots of W22, respectively. *zmhipp* (S) and *zmhipp* (R) represent the shoots and roots of the mutant *zmhipp*, respectively.

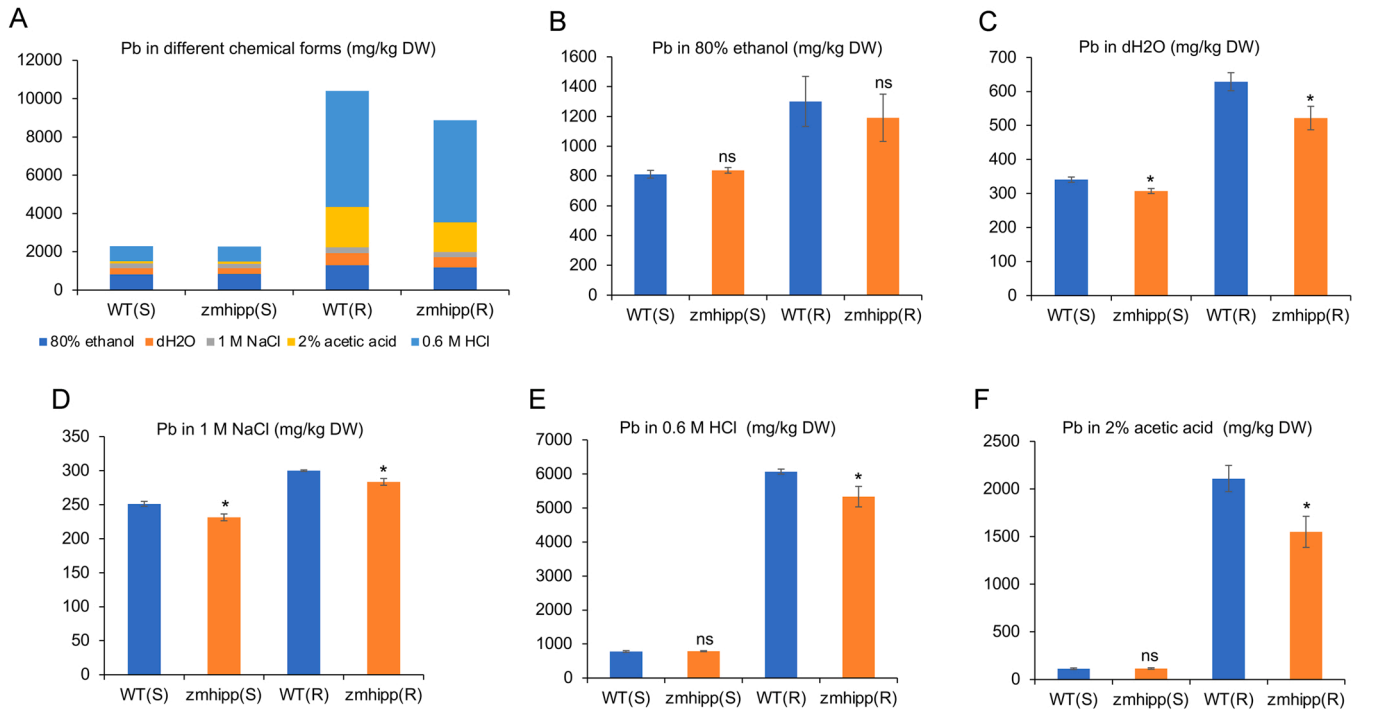

Fig. 6. Comparison of Pb content in various chemical forms between the wild-type line W22 and the mutant *zmhipp*. (A) Overall Pb content in different chemical forms. (B) Pb concentration in 80% ethanol. (C) Pb concentration in dH_2O. (D) Pb concentration in 1 M NaCl. (E) Pb concentration in 0.6 M HCl. (F) Pb concentration in 2% acetic acid. ns represents no significance ($P > 0.05$) between W22 and *zmhipp*. * denotes significant difference between W22 and *zmhipp* at $P < 0.05$ level. WT (S) and WT (R) represent the shoots and roots of the wild-type W22, respectively. *zmhipp* (S) and *zmhipp* (R) represent the shoots and roots of the mutant *zmhipp*, respectively.

content in the WT shoots resulted from increased organic Pb (extracted by dH_2O), Pb pectates, protein-integrated Pb, and adsorptive Pb (Fig. 6C, D).

In both the WT and mutant lines, most of the Pb was distributed in the subcellular level F1 (cell walls and relative debris) (Fig. 7A). Approximately 81.40–83.52% and 53.87–64.96% of Pb were present in F1 of the roots and shoots, respectively, for the two lines (Fig. 7A). Conversely, Pb in F2 (cell membrane and organelles) accounted for the lowest proportion of total Pb in both lines, with 6.50–7.72% in the roots and 13.59–20.66% in the shoots (Fig. 7A). The concentration of Pb in each form (F1, F2, and F3) was significantly ($P < 0.05$) higher in the roots of the WT line than in those of the mutant line (Fig. 7B, C, D). Notably, Pb in the F1 component had significantly ($P < 0.05$) increased to 1596.66 mg/kg DW in the WT shoots, compared to 1035.03 mg/kg DW in the mutant shoots (Fig. 7B). In contrast, Pb in the F2 component had significantly ($P < 0.05$) decreased to 303.00 mg/kg DW in the WT shoots compared to 397.02 mg/kg DW of the mutant shoots (Fig. 7C). This suggested that *ZmHIPP* facilitates Pb deposition in the cell wall and inhibits its penetration into the cell organelles, thereby alleviating Pb toxicity in the maize seedlings.

4. Discussion

4.1. ZmHIPP is a positive regulatory factor for Pb tolerance and accumulation across species

This study reported a heavy metal tolerance-associated protein, *ZmHIPP*, that confers Pb tolerance to maize seedlings by increasing the deposition of Pb in the cell wall and alleviating Pb toxicity. The heterologous expression of *ZmHIPP* in the Pb-sensitive mutant of yeast complemented the Pb tolerance of the mutant and enhanced Pb absorption into yeast cells. Overexpression of *ZmHIPP* in Arabidopsis promoted its growth under Pb treatment. Knockdown of *ZmHIPP* in maize significantly decreased Pb tolerance in the seedlings and reduced Pb accumulation in the entire plant. Compared to that in the maize mutant *zmhipp*, increased Pb content in the WT plants was mainly due to low-toxicity Pb forms. Additionally, we showed that *ZmHIPP* alleviates Pb toxicity in maize by transporting Pb to the cell wall. *ZmHIPP* encodes an HMA isoprenylated plant protein. HMA is a conserved domain in many proteins and can transport or detoxify heavy metals (Leng et al., 2019). However, further studies are required to verify whether *ZmHIPP* is associated with the tolerance of other heavy metals. We found that hundreds of genes in other plants were orthologs of *ZmHIPP*, including three genes (*Sobic.005G033700*, *Sobic.005G033400*, and *Sobic.005G033600*) from sorghum that showed a close phylogenetic relationship with *ZmHIPP* (Fig. S4). Therefore, the three sorghum genes probably regulate heavy metal tolerance in sorghum.

4.2. Combined QTL mapping and WGCNA is an effective strategy for identifying key genes that control heavy metal tolerance in plants

Linkage mapping is an effective method for understanding the genetic architecture of quantitative traits (Tanksley, 1993) and has been widely used to identify the genomic regions controlling abiotic stress-tolerant traits in various species (Deniau et al., 2006; Courbot et al., 2007; Hou et al., 2021). Deniau et al. (2006) mapped the QTL responsible for Zn and Cd accumulation in the heavy metal hyperaccumulator *Thlaspi caerulescens* using a parental F2 population (Deniau et al., 2006). The phenotypic variance explained by the mapped QTL ranged from 23.8% to 60.4%, with several common QTL detected between Zn and Cd concentrations in the roots (Deniau et al., 2006). In Arabidopsis, three QTL were identified for Cd tolerance using a BC1 population, contributing 43%, 24%, and 16% of the phenotypic variance (Courbot et al., 2007). The IBM Syn 10 DH population was previously used to dissect 64 QTL for the combined tolerance of Pb and Cd stress in maize (Hou et al., 2021). However, due to the larger intervals of the mapped QTL, fine-mapping based on enlarged recombinant populations is required for cloning the causal genes of the target traits (Han et al.,

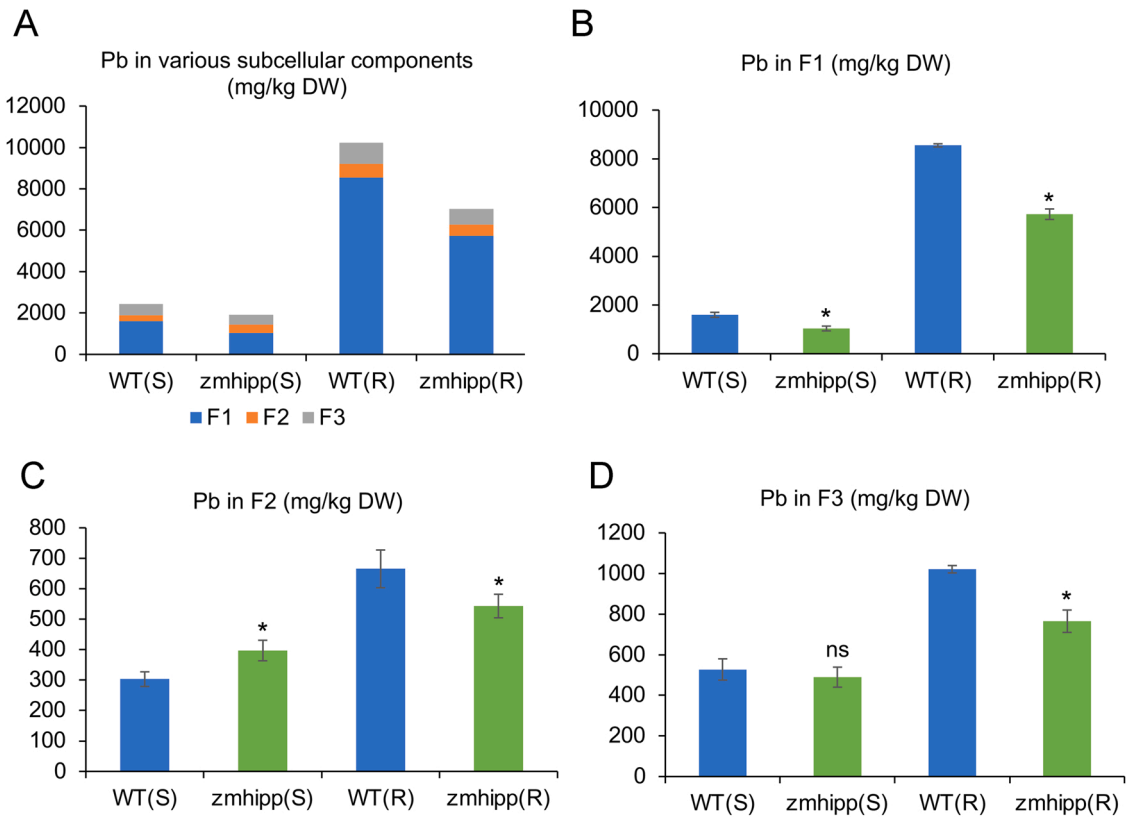

Fig. 7. Comparison of Pb content in different subcellular components between the wild-type line W22 and the mutant *zmhipp*. (A) Overall Pb content in different subcellular components. (B) Pb concentration in F1 (cell walls and relative debris). (C) Pb concentration in F2 (cell membrane and organelles). (D) Pb concentration in F3 (cytosol and cytoplasm). ns represents no significance ($P > 0.05$) between W22 and *zmhipp*. * denotes significant difference between W22 and *zmhipp* at $P < 0.05$ level. WT (S) and WT (R) represent the shoots and roots of the wild-type line W22, respectively. *zmhipp* (S) and *zmhipp* (R) represent the shoots and roots of the mutant *zmhipp*, respectively.

2020). Based on a major QTL for Cd accumulation in maize, the candidate gene *ZmHMA3* was fine-mapped using an F2 population of 305 individuals. It was further validated using maize mutant strategies to control Cd accumulation in maize grains (Tang et al., 2021). However, determining the causal genes by QTL fine-mapping is very time-consuming and expensive.

The recently developed WGCNA facilitates the identification of hub genes that control target traits based on gene expression patterns (Langfelder and Horvath, 2008). In this study, we combined linkage mapping and WGCNA to clone the key genes affecting Pb tolerance in maize seedlings. By QTL mapping, we detected five QTL responsible for the LTCs of maize seedlings and identified 267 gene models in these QTL intervals. According to the RNA-seq data, 82 of the 267 genes were responsive to Pb treatment. Using WGCNA, we clustered the 82 genes into different co-expression modules based on the normalized expression value of each gene. From the correlation between each module and Pb-tolerant phenotypes, the blue module, with 18 co-expressed gene models, was selected as the model associated with Pb tolerance. Seven of the eighteen genes showed the highest values for eigengene connectivity and weight, and were identified as the hub genes controlling Pb tolerance. Therefore, we were able to efficiently identify the potential functional genes for Pb tolerance by the combined use of QTL and WGCNA. This strategy circumvented the process of QTL fine-mapping and saved considerable time and cost.

4.3. Variation in the ZmHIPP promoter regulates Pb tolerance probably by affecting its binding with the GRAS transcription factor

Promoters are key cis-acting elements of functional genes that play a crucial role in controlling gene expression at the transcriptional level (Hernandez-Garcia and Finer, 2014). Natural variations in gene promoters affect gene expression levels and regulate growth and development (Zhao et al., 2018), amino acid levels (Sun et al., 2020), grain yield (Duan et al., 2017), stress tolerance (Ye et al., 2018; Jin et al., 2021), and heavy metal accumulation (Liu et al., 2020) in plant species. In rice, an 11-nucleotide change in the promoter of *OsHMA3* resulted in a disparity in the *OsHMA3* expression levels and contributed to distinct Cd accumulation in the grains of two lines (Liu et al., 2020). We conducted a *ZmHIPP*-based association analysis to illustrate how the variations in *ZmHIPP* sequence controlled phenotypic variations in Pb tolerance. One SNP (S2_149356641, A/G), located in the promoter of *ZmHIPP*, was significantly associated with the LTCs of maize seedlings. Under Pb treatment, the lines with "A" allele had higher LTCs and *ZmHIPP* expression level than those with "G." Notably, the SNP S2_149356641 was closely linked to a GRAS transcription factor binding motif (GAAAAGAAAACATAAAAAAT) in the promoter. In the "A" haplotype, a complete GRAS-binding motif was included in the promoter of *ZmHIPP*. However, this motif was mutated to "GAAAAGAAAACATAAAGAAT" in the "G" haplotype, likely preventing the GRAS transcription factor from binding. The GRAS transcription factor family is specific to plant species and plays a significant role in various physiological processes, including regulation of abiotic stress tolerance (Yuan et al., 2016; Li et al., 2018b; Fan et al., 2021; Zhang et al., 2020, 2021c). The "A"-type lines had the exact GRAS binding motif on the *ZmHIPP* promoter, which could successfully bind the GRAS transcription factors. The expression of *ZmHIPP* was efficiently promoted by GRAS proteins in the "A"-type lines. In contrast, the expression of *ZmHIPP* could not be activated in the "G"-type lines due to mutation of the GRAS-binding motif in the *ZmHIPP* promoter. This evidence could explain the difference in Pb tolerance between the two haplotypes.

4.4. Increasing the expression of ZmHIPP in maize is a potential method for bioremediation of Pb-polluted soil

Excess of heavy metals in soil is a public concern because they can enter the human body via the food chain. The development of heavy metal hyperaccumulators is a practical approach for the bioremediation of heavy metal-polluted soil (Rascio and Navari-Izzo, 2011). As a major crop in the world, maize can potentially serve as a Pb hyperaccumulator crop because of greater biomass than other plants. Currently, the kernels and non-edible parts of maize have been used as raw materials for energy generation. This provides the promising use of *ZmHIPP*-transgenic maize in soil bioremediation. We have shown that *ZmHIPP* contributes positively to Pb absorption from the environment and Pb tolerance in maize. Therefore, in the future, increasing *ZmHIPP* expression in maize using transgenic approaches can potentially enhance its Pb absorption ability (from soil) and aid in the bioremediation of Pb-polluted soil.

5. Conclusion

We characterized the novel Pb tolerance-associated gene *ZmHIPP* from maize for the first time. Overexpression and mutation studies revealed that *ZmHIPP* is a positive regulatory factor for Pb tolerance. *ZmHIPP* enhanced Pb deposition in the cell wall and alleviated Pb toxicity in maize seedlings. These findings broaden our knowledge of Pb tolerance mechanisms in plants and provide new insights into the bioremediation of Pb-polluted soil.

CRediT authorship contribution statement

YS conceived the project and designed the experiments. LM and RA performed most of the experiments and data analysis. LJ, CZ, ZL, CYZ, and CY participated in some of the experiments. YS and LM drafted the manuscript with the contributions from GP and TL. All the authors reviewed and approved the final manuscript.

Declaration of Competing Interest

The authors declare that they have no known competing financial interests or personal relationships that could have appeared to influence the work reported in this paper.

Data Availability

The raw data generating from 42 samples used in this study were deposited in Genome Sequence Archive (GSA) in National Genomics Data Center (NGDC) database with the accession number CRA004789.

Acknowledgements

This work is supported by the National Key Research and Development Program of China (2021YFF1000303), the National Nature Science Foundation of China (31871637 and 32072073), and the Sichuan Science and Technology Program (2021JDTD0004 and 2021YJ0476). These authors thank Prof. Micheal Lee at Iowa State University for providing the IBM Syn10 DH population. These authors also thank Editage (www.editage.cn) for English language editing.

Appendix A. Supporting information

Supplementary data associated with this article can be found in the online version at doi:10.1016/j.jhazmat.2022.128457.

References

de Abreu-Neto, J.B., Turchetto-Zolet, A.C., de Oliveira, L.F., Zanettini, M.H., Margis-Pinheiro, M., 2013. Heavy metal-associated isoprenylated plant protein (HIPP): characterization of a family of proteins exclusive to plants. FEBS J. 280, 1604–1616.
Antonovics, J., Bradshaw, A.D., Turner, R.G., 1971. Heavy metal tolerance in plants. Adv. Ecol. Res. 7, 1–85 (Academic Press).
Buckler, E.S., Stevens, N.M., 2006. Maize origins, domestication, and selection. In: Motley, T.J., Zerega, N., Cross, H. (Eds.), Darwin's Harvest. Columbia University Press, pp. 67–90.
Cao, S., Chen, Z., Liu, G., Jiang, L., Yuan, H., Ren, G., Bian, X., et al., 2009. The Arabidopsis Ethylene-Insensitive 2 gene is required for lead resistance. Plant Physiol. Bioch 47, 308–312.
Clough, S., Bent, A., 2010. Floral dip: a simplified method for Agrobacterium-mediated transformation of Arabidopsis thaliana. Plant J. 16, 735–743.
Collin, V.C., Eymery, F., Genty, B., Rey, P., Havaux, M., 2008. Vitamin E is essential for the tolerance of Arabidopsis thaliana to metal-induced oxidative stress. Plant Cell Environ. 31, 244–257.
Courbot, M., Willems, G., Motte, P., Arvidsson, S., Roosens, N., Saumitou-Laprade, P., Verbruggen, N., 2007. A major quantitative trait locus for cadmium tolerance in Arabidopsis halleri colocalizes with HMA4, a gene encoding a heavy metal ATPase. Plant Physiol. 144, 1052–1065.
Cox, M.S., Bell, P.F., Kovar, J.L., 1996. Differential tolerance of canola to arsenic when grown hydroponically or in soil. J. Plant Nutr. 19, 1599–1610.
Deniau, A.X., Pieper, B., Ten Bookum, W.M., Lindhout, P., Aarts, M.G.M., Schat, H., 2006. QTL analysis of cadmium and zinc accumulation in the heavy metal hyperaccumulator Thlaspi caerulescens. Theor. Appl. Genet 113, 907–920.
Dey, S.K., Dey, J., Patra, S., Pothal, D., 2007. Changes in the antioxidative enzyme activities and lipid peroxidation in wheat seedlings exposed to cadmium and lead stress. Braz. J. Plant Physiol. 19, 53–60.
Dietz, K.J., Mittler, R., Noctor, G., 2016. Recent progress in understanding the role of reactive oxygen species in plant cell signaling. Plant Physiol. 171, 1535.
Ding, D., Li, W., Song, G., Qi, H., Liu, J., Tang, J., 2011. Identification of QTLs for arsenic accumulation in maize (Zea mays L.) using a RIL Population. PLoS One 6, e25646.
Duan, P., Xu, J., Zeng, D., Zhang, B., Geng, M., Zhang, G., Huang, K., et al., 2017. Natural variation in the promoter of *GSE5* contributes to grain size diversity in rice. Mol. Plant 10, 685–694.
Ewais, E.A., 1997. Effects of cadmium, nickel and lead on growth, chlorophyll content and proteins of weeds. Biol. Plant. 39, 403–410.
Fan, T., Yang, L., Wu, X., Ni, J., Jiang, H., Zhang, Q., Fang, L., et al., 2016. The *PSE1* gene modulates lead tolerance in Arabidopsis. J. Exp. Bot. 67, 4685–4695.
Fan, Y., Yan, J., Lai, D., Yang, H., Xue, G., He, A., Guo, T., et al., 2021. Genome-wide identification, expression analysis, and functional study of the GRAS transcription factor family and its response to abiotic stress in sorghum [Sorghum bicolor (L.) Moench]. BMC Genom. 22, 1–21.
Farthing, E.C., Menguer, P.K., Fett, J.P., Williams, L.E., 2017. OsMTP11 is localised at the Golgi and contributes to Mn tolerance. Sci. Rep. 7, 1–13.
Fu, Z., Li, W., Zhang, Q., Wang, L., Zhang, X., Song, G., Fu, Z., et al., 2014. Quantitative trait loci for mercury accumulation in maize (Zea mays L.) identified using a RIL population. PLoS One 9, e107243.
Fu, Z., Li, W., Xing, X., Xu, M., Liu, X., Li, H., Xue, Y., 2016. Genetic analysis of arsenic accumulation in maize using QTL mapping. Sci. Rep. 6, 1–8.
Gao, J., Zhang, Y., Lu, C., Peng, H., Luo, M., Li, G., Shen, Y., et al., 2015. The development dynamics of the maize root transcriptome responsive to heavy metal Pb pollution. Biochem. Biophys. Res. Commun. 458, 287–293.
Gisbert, C., Ros, R., De Haro, A., Walker, D.J., Pilar Bernal, M., Serrano, R., Navarro-Aviñó, J., 2003. A plant genetically modified that accumulates Pb is especially promising for phytoremediation. Biochem. Bioph. Res. Co. 303, 440–445.
Godfray, H.C., Beddington, J.R., Crute, I.R., Haddad, L., Lawrence, D., Muir, J.F., Pretty, J., et al., 2010. Food security: the challenge of feeding 9 billion people. Science 327, 812–818.
Han, X., Qin, Y., Sandrine, A.M.N., Qiu, F., 2020. Fine mapping of *qKRN8*, a QTL for maize kernel row number, and prediction of the candidate gene. *Theor. Appl. Genet.* 133, 3139–3150.
Hasan, S.A., Fariduddin, Q., Ali, B., Hayat, S., Ahmad, A., 2009. Cadmium: toxicity and tolerance in plants. J. Environ. Biol. 30, 165–174.
Hernandez-Garcia, C.M., Finer, J.J., 2014. Identification and validation of promoters and cis-acting regulatory elements. Plant Sci. 217, 109–119.
Holland, S.L., Reader, T., Dyer, P.S., Avery, S.V., 2013. Phenotypic heterogeneity is a selected trait in natural yeast populations subject to environmental stress. Environ. Microbiol. 16, 1729–1740.
Hong, C., Cheng, D., Zhang, G., Zhu, D., Chen, Y., Tan, M., 2017. The role of *ZmWRKY4* in regulating maize antioxidant defense under cadmium stress. Biochem. Biophys. Res. Commun. 482, 1504–1510.
Hou, F., Zhou, X., Liu, P., Yuan, G., Zou, C., Lübberstedt, T., Pan, G., et al., 2021. Genetic dissection of maize seedling traits in an IBM Syn10 DH population under the combined stress of lead and cadmium. Mol. Genet. Genom. 296, 1057–1070.
Huang, C.F., Yamaji, N., Mitani, N., Yano, M., Nagamura, Y., Ma, J.F., 2009. A bacterial-type ABC transporter is involved in aluminum tolerance in rice. Plant Cell 21, 655–667.
Jansen, C., Zhang, Y., Liu, H., Gonzalez-Portilla, P.J., Lauter, N., Kumar, B., Trucillo-Silva, I., et al., 2015. Genetic and agronomic assessment of cob traits in corn under low and normal nitrogen management conditions. Theor. Appl. Genet. 128, 1231–1242.

Jin, T., Sun, Y., Shan, Z., He, J., Wang, N., Gai, J., Li, Y., 2021. Natural variation in the promoter of GsERD15B affects salt tolerance in soybean. Plant Biotechnol. J. 19, 1155–1169.
Kim, D.Y., Bovet, L., Maeshima, M., Martinoia, E., Lee, Y., 2007. The ABC transporter AtPDR8 is a cadmium extrusion pump conferring heavy metal resistance. Plant J. 50, 207–218.
Koike, S., Inoue, H., Mizuno, D., Takahashi, M., Nakanishi, H., Mori, S., Nishizawa, N.K., 2004. OsYSL2 is a rice metal-nicotianamine transporter that is regulated by iron and expressed in the phloem. Plant J. 39, 415–424.
Kulich, I., Vojtíková, Z., Glanc, M., Ortmannová, J., Rasmann, S., Žárský, V., 2015. Cell wall maturation of Arabidopsis trichomes is dependent on exocyst subunit EXO70H4 and involves callose deposition. Plant Physiol. 168, 120–131.
Lander, E., Kruglyak, L., 1995. Genetic dissection of complex traits: guidelines for interpreting and reporting linkage results. Nat. Genet. 11, 241–247.
Langfelder, P., Horvath, S., 2008. WGCNA: an R package for weighted correlation network analysis. BMC Bioinforma. 9, 559.
Lee, M., Lee, K., Lee, J., Noh, E.W., Lee, Y., 2005. AtPDR12 contributes to lead resistance in Arabidopsis. Plant Physiol. 138, 827–836.
Leng, F., Li, Y., Luo, W., Wei, Q., Jing, Y., Wang, X., Yang, M., et al., 2019. Cloning, expression, and bioinformatics analysis of heavy metal resistance gene *afe*_1862 from Acidithiobacillus ferrooxidans L1 in Escherichia coli. Biol. Trace Elem. Res. 189, 291–300.
Li, C., Wang, Y., Liu, L., Hu, Y., Zhang, F., Mergen, S., Wang, G., et al., 2011. A rice plastidial nucleotide sugar epimerase is involved in galactolipid biosynthesis and improves photosynthetic efficiency. PLoS Genet. 7, e1002196.
Li, J., Zhao, C., Wei, L., Li, X., Liu, F., Zhang, M., Liu, X., et al., 2018a. Preservation of cichoric acid antioxidant properties loaded in heat treated lactoferrin nanoparticles. Molecules 23, 2678.
Li, P., Zhang, B., Sun, T., Li, P., Xin, X., Wang, W., Zhao, X., et al., 2018b. BrLAS, a GRAS transcription factor from Brassica rapa, is involved in drought stress tolerance in transgenic Arabidopsis. Front. Plant Sci. 9, 1792.
Li, P., Yang, X., Wang, H., Pan, T., Wang, Y., Xu, Y., Xu, C., 2021. Genetic control of root plasticity in response to salt stress in maize. Theor. Appl. Genet. 134, 1475–1492.
Lippmann, M., 1990. Alice Hamilton lecture. lead and human health: background and recent findings. Environ. Res. 51, 1–24.
Liu, C.-L., Gao, Z.-J., Shang, L.-G., Yang, C.-H., Ruan, B.-P., Zeng, D.-L., Guo, L.-B., et al., 2020. Natural variation in the promoter of OsHMA3 contributes to differential grain cadmium accumulation between Indica and Japonica rice. J. Integr. Plant Biol. 62, 314–329.
Ma, L., Guan, Z., Zhang, Z., Zhang, X., Zhang, Y., Zou, C., Peng, H., et al., 2018. Identification of quantitative trait loci for leaf-related traits in an IBM Syn10 DH maize population across three environments. Plant Breed. 137, 127–138.
Ma, L., Qing, C., Frei, U., Shen, Y., Lübberstedt, T., 2020. Association mapping for root system architecture traits under two nitrogen conditions in germplasm enhancement of maize doubled haploid lines. Crop J. 8, 213–226.
Ma, L., Zhang, M., Chen, J., Qing, C., He, S., Zou, C., Yuan, G., et al., 2021. GWAS and WGCNA uncover hub genes controlling salt tolerance in maize (Zea mays L.) seedlings. Theor. Appl. Genet. 134, 3305–3318.
Ma, M., Lau, P.S., Jia, Y.T., Tsang, W.K., Lam, S.K., Tam, N.F., Wong, Y.S., 2003. The isolation and characterization of Type 1 metallothionein (MT) cDNA from a heavy-metal-tolerant plant, *Festuca rubra* cv. Merlin. Plant Sci. 164, 51–60.
Magalhaes, J.V., Liu, J., Guimarães, C.T., Lana, U.G., Alves, V.M., Wang, Y.H., Schaffert, R.E., et al., 2007. A gene in the multidrug and toxic compound extrusion (MATE) family confers aluminum tolerance in sorghum. Nat. Genet. 39, 1156–1161.
Mao, Q.Q., Guan, M.Y., Lu, K.X., Du, S.T., Fan, S.K., Ye, Y.-Q., Lin, X.Y., 2014. Inhibition of nitrate transporter 1.1-controlled nitrate uptake reduces cadmium uptake in Arabidopsis. Plant Physiol. 166, 934–944.
Nagajyoti, P.C., Lee, K.D., Sreekanth, T.V.M., 2010. Heavy metals, occurrence and toxicity for plants: a review. Environ. Chem. Lett. 8, 199–216.
Obroucheva, N.V., Bystrova, E.I., Ivanov, V.B., Antipova, O.V., Seregin, I.V., 1998. Root growth responses to lead in young maize seedlings. In: Box Jr., James, E. (Eds.), Root Demographics and Their Efficiencies in Sustainable Agriculture, Grasslands and Forest Ecosystems. Springer, Dordrecht, pp. 445–456.
Pace, J., Lee, N., Naik, H.S., Ganapathysubramanian, B., Lübberstedt, T., 2014. Analysis of maize (Zea mays L.) seedling roots with the high-throughput image analysis tool ARIA (Automatic Root Image Analysis). PLoS One 9, e108255.
Pace, J., Gardner, C., Romay, C., Ganapathysubramanian, B., Lübberstedt, T., 2015. Genome-wide association analysis of seedling root development in maize (Zea mays L.). BMC Genom. 16, 47.
Passow, H., Rothstein, A., Clarkson, T.W., 1961. The general pharmacology of heavy metals. Pharmac. Rev. 13, 185–224.
Raihan, M.S., Liu, J., Huang, J., Gao, H., Pan, Q., Yan, J., 2016. Multi-environment QTL analysis of grain morphology traits and fine mapping of a kernel-width QTL in Zheng58 × SK maize population. Theor. Appl. Genet. 129, 1465–1477.
Rascio, N., Navari-Izzo, F., 2011. Heavy metal hyperaccumulating plants: how and why do they do it? And what makes them so interesting? Plant Sci. 180, 169–181.
Shannon, P., Markiel, A., Ozier, O., Baliga, N.S., Wang, J.T., Ramage, D., Amin, N., et al., 2003. Cytoscape: a software environment for integrated models of biomolecular interaction networks. Genome Res. 13, 2498–2504.
Shen, Y., Zhang, Y., Chen, J., Lin, H., Zhao, M., Peng, H., Liu, L., 2013. Genome expression profile analysis reveals important transcripts in maize roots responding to the stress of heavy metal Pb. Physiol. Plant. 147, 270–282.
Sun, Y., Shi, Y., Liu, G., Yao, F., Zhang, Y., Yang, C., Guo, H., 2020. Natural variation in the OsbZIP18 promoter contributes to branched-chain amino acid levels in rice. N. Phytol. 228, 1548–1558.
Tang, B., Luo, M., Zhang, Y., Guo, H., Li, J., Song, W., Zhang, R., et al., 2021. Natural variations in the P-type ATPase heavy metal transporter *ZmHMA3* controlling cadmium accumulation in maize grains. J. Exp. Bot. 3, erab254.
Tanksley, S.D., 1993. Mapping polygenes. Annu. Rev. Genet. 27, 205–233.
Tehseen, M., Cairns, N., Sherson, S., Cobbet, C.S., 2010. Metallochaperone-like genes in *Arabidopsis thaliana*. Metallomics 2, 556–564.
Tsugama, D., Liu, S., Takano, T., 2013. Metal-binding ability of VIP1: a bZIP protein in *Arabidopsis thaliana*. Protein J. 32, 526–532.
Tung, G., Temple, P.J., 1996. Uptake and localization of lead in corn (*Zea mays* L.) seedlings, a study by histochemical and electron microscopy. Sci. Total Environ. 188, 71–85.
van de Mortel, J.E., Schat, H., Moerland, P.D., Ver Loren van Themaat, E., van der Ent, S., Blankestijn, H., Ghandilyan, A., et al., 2008. Expression differences for genes involved in lignin, glutathione and sulphate metabolism in response to cadmium in Arabidopsis thaliana and the related Zn/Cd-hyperaccumulator Thlaspi caerulescens. Plant Cell Environ. 31, 301–324.
Wang, S., Basten, C., Zeng, Z., 2012. Windows QTL cartographer 2.5. Department of Statistics, North Carolina State University, Raleigh, NC.
Wang, X., Liu, Y., Zeng, G., Chai, L., Song, X., Min, Z., Xiao, X., 2008. Subcellular distribution and chemical forms of cadmium in Bechmeria nivea (L.) Gaud. Environ. Exp. Bot. 62, 389–395.
Wang, Y., Shen, H., Xu, L., Zhu, X., Li, C., Zhang, W., Xie, Y., et al., 2015.) Transport, ultrastructural localization, and distribution of chemical forms of lead in radish (*Raphanus sativus* L.). Front. Plant. Sci. 6, 293.
Weigel, H.J., Jäger, H.J., 1980. Subcellular distribution and chemical form of cadmium in bean plants. Plant Physiol. 65, 480–482.
Wen, W., Li, D., Li, X., Gao, Y., Li, W., Li, H., Liu, J., et al., 2014. Metabolome-based genome-wide association study of maize kernel leads to novel biochemical insights. Nat. Commun. 5, 1–10.
Xiao, S., Gao, W., Chen, Q.-F., Ramalingam, S., Chye, M.-L., 2008. Overexpression of membrane-associated acyl-CoA-binding protein ACBP1 enhances lead tolerance in Arabidopsis. Plant J. 54, 141–151.
Xu, J.L., Song, W.C., Bao, Z.P., Yang, J.R., Liu, H., 1991. Chemical forms of Pb, Cd and Cu in crops. Chin. J. Appl. Ecol. 2, 244–248.
Xu, P.X., Wang, Z.L., 2013. Physiological mechanism of hypertolerance of cadmium in Kentucky bluegrass and tall fescue: chemical forms and tissue distribution. Environ. Exp. Bot. 96, 35–42.
Xu, Z.M., Mei, X.Q., Tan, L., Li, Q.S., Wang, L.L., He, B.Y., Guo, S.H., et al., 2018. Low root/shoot (R/S) biomass ratio can be an indicator of low cadmium accumulation in the shoot of Chinese flowering cabbage (Brassica campestris L. ssp. chinensis var. utilis Tsen et Lee) cultivars. Environ. Sci. Pollut. Res. Int. 25, 36328–36340.
Yang, N., Liu, J., Gao, Q., Gui, S., Chen, L., Yang, L., Huang, J., et al., 2019. Genome assembly of a tropical maize inbred line provides insights into structural variation and crop improvement. Nat. Genet. 51, 1052–1059.
Yang, Y.-Y., Jung, J.-Y., Song, W.-Y., Suh, H.-S., Lee, Y., 2000. Identification of rice varieties with high tolerance or sensitivity to lead and characterization of the mechanism of tolerance. Plant Physiol. 124, 1019–1026.
Ye, N.-H., Wang, F.-Z., Shi, L., Chen, M.-X., Cao, Y.-Y., Zhu, F.-Y., Wu, Y.-Z., et al., 2018. Natural variation in the promoter of rice calcineurin B-like protein10 (OsCBL10) affects flooding tolerance during seed germination among rice subspecies. Plant J. 94, 612–625.
Yuan, Y., Fang, L., Karungo, S.K., Zhang, L., Gao, Y., Li, S., Xin, H., 2016. Overexpression of *VaPAT1*, a GRAS transcription factor from *Vitis amurensis*, confers abiotic stress tolerance in Arabidopsis. Plant Cell Rep. 35, 655–666.
Zhang, H., Liu, X., Wang, X., Sun, M., Song, R., Mao, P., Jia, S., 2021c. Genome-wide identification of GRAS gene family and their responses to abiotic stress in Medicago sativa. Int. J. Mol. Sci. 22, 7729.
Zhang, S., Li, X., Fan, S., Zhou, L., Wang, Y., 2020. Overexpression of *HcSCL13*, a Halostachys caspica GRAS transcription factor, enhances plant growth and salt stress tolerance in transgenic Arabidopsis. Plant Physiol. Biochem. 151, 243–254.
Zhang, X., Liu, P., Qing, C., Yang, C., Shen, Y., Ma, L., 2021a. Comparative transcriptome analyses of maize seedling root responses to salt stress. PeerJ 9, e10765.
Zhang, Y., Ge, F., Hou, F., Sun, W., Zheng, Q., Zhang, X., Ma, L., et al., 2017. Transcription factors responding to Pb stress in maize. Genes 8, 231.
Zhang, Y., Liu, P., Wang, C., Zhang, N., Zhu, Y., Zou, C., Yuan, G., et al., 2021b. Genome-wide association study uncovers new genetic loci and candidate genes underlying seed chilling-germination in maize. PeerJ 9, e11707.
Zhao, L., Li, M., Xu, C., Yang, X., Li, D., Zhao, X., Wang, K., 2018. Natural variation in GmGBP1 promoter affects photoperiod control of flowering time and maturity in soybean. Plant J. 96, 147–162.
Zhou, X.Y., Qiu, R.L., Hu, P.J., Li, Q.F., Zhang, T., Yu, F.M., Zhao, X., 2008. Effects of cadmium and lead on subcellular distribution and chemical form of zinc in Potentilla griffithii var. velutina. Environ. Sci. 29, 2028–2036.